How Different are the Crystal Structures of Chiral and Racemic Diacylphosphatidylethanolamines?

Douglas L. Dorset

Electron Diffraction Department, Medical Foundation of Buffalo, Inc., 73 High Street, Buffalo, New York 14203, U.S.A.

Z. Naturforsch. **43c**, 319–327 (1988); received November 20, 1987

Phospholipids, X-Ray Diffraction, Electron Diffraction

Both chiral and racemic phosphatidylethanolamines are known to crystallize in a similar polymorphic form with nearly the same lamellar spacing; yet published lamellar X-ray diffraction intensity data for those materials do not agree with one another, even though the peak positions in Patterson maps are nearly the same. Translational structural searches based on the crystal structure of the racemic compound also lead to similar packing models with both data sets, although the agreement between model and observed data is poor for the chiral compound. A separate analysis of L-DMPE based on lamellar electron diffraction data again leads to a similar lamellar structure with a better agreement between calculated and observed structure factors. The major difference seen for enantiomeric *vs.* racemic compounds is that, for the racemic lipid, the lateral unit cell spacings are about 3% larger than the chiral form, perhaps indicating a more stable hydrogen bonding network, in agreement with the higher melting point of the racemic compound. Attempts to explain this difference with other head group conformations, however, have not yet produced an improved structural model.

Introduction

Although the chirality of many lipids containing the 1,2-diacylglycerol moiety is expressed by a rather small region of the molecular structure, its influence on the overall packing of the molecules in the crystalline state is not fully understood. One aspect of the problem is whether or not a racemic mixture would crystallize in a fashion similar to the optically active crystal – *i.e.* in general whether or not a continuous solid solution could be formed between the mirror-related molecules in the racemate. As discussed by Kitaigorodskii [1], for continuous solid solubility to occur, the molecular shape and volume of the two species must be similar enough to overcome the packing constraints imposed by the presence of oppositely-handed molecules; hence the molecular array in a solid solution is merely pseudo-racemic. Otherwise, fractionation occurs, producing either a simple eutectic with a melting point minimum at the 1:1 composition (*i.e.* a two-phase mixture) or a molecular compound with a melting point maximum at this composition, the latter being most characteristic of a true racemate.

For the 1,2-diacylglycerol lipids, the phase behavior of racemic mixtures is quite variable. The 1,2-diglycerides, for example, do not form solid solutions in the crystalline β'_L-form, nor is there any evidence for racemic compound formation [2] – thus the eutectic must be composed of a mechanical mixture of chiral crystals. These restrictions are relaxed as soon as the compounds are converted to the lower melting α_L-form for which continuous solid solutions are permitted [2]. Two types of fractionation behavior are noted for phospholipids. Addition of the D-enantiomer of a diacylphosphatidylcholine to the L-form causes gradual disappearance of a DSC subtransition due to the L_c phase – even in fully hydrated multilamellar vesicles [3]. Single crystals can be grown for the DL-form, however, but they are quite different from the L-form crystals and exhibit different hydration behavior [4, 5].

Evidence has been found for the existence of a true racemic compound in the case of 1,2-diacylphosphatidylethanolamine, *i.e.* melting points of the racemic mixtures are higher than that of the chiral compound [6]. The crystal structure of 1,2-dilauroyl-*rac*-glycerophosphoethanolamine [7] is centrosymmetric, also consistent with the formation of a true racemic compound. Whether or not the formation of a molecular compound involves a conformational change of the molecule or any other difference in molecular packing from that found in the chiral crystals, however, is not yet clear.

In the analysis of lamellar packing for 1,2-dimyristoyl-*rac*-glycerophosphoethanolamine, Hitchcock *et al.* [8] showed that the molecular conformation of

Verlag der Zeitschrift für Naturforschung, D-7400 Tübingen
0341–0382/88/0500–0319 $ 01.30/0

the 1,2-dilauroyl homolog is retained despite the absence of the acetic acid solvent molecule included in the original crystal structure [7]. A comparison of lamellar spacings for chiral and racemic phosphatidylethanolamines [9], moreover, indicates that no significant difference exists in this long unit cell spacing for corresponding crystal forms. On the other hand, a recent structure analysis of 1,2-dimyristoyl-*sn*-glycerophosphoethanolamine based on lamellar X-ray diffraction data [10] proposes that a conformational difference may indeed be found in the head group region of the chiral form.

Since no direct comparison of the X-ray data from the chiral compound has been made to the model based on the racemic crystal structure, the relation between the two crystal forms is explored further in this paper to seek evidence for a significant change in molecular orientation. These studies are also supported by electron diffraction studies on epitaxially crystallized samples of the chiral form.

Materials and Methods

Crystallization and swelling of crystal lamellae

Samples of the lipid 1,2-dimyristoyl-*sn*-glycerophosphoethanolamine were purchased from Calbiochem-Behring (La Jolla, Cal.) and used without further purification. As in a study of the racemic 1,2-dipalmitoyl homolog [11], plate-like crystals used for characterization of the methylene subcell were grown on carbon-film-covered Cu electron microscope grids by evaporation of a dilute solution of the lipid in cyclohexane. Epitaxially crystallized samples were prepared on naphthalene following the procedure of Wittmann and Manley [12] as often described before [13]. In this crystal growth, the long unit cell axes are parallel to a major crystal face rather than perpendicular to it and thus one can directly obtain 00ℓ electron diffraction patterns due to the lamellar repeat.

Swelling experiments for the epitaxially crystallized samples were carried out in a fashion similar to that described by Suwalsky and Duk [10]. Supersaturated solutions of $MgCl_2 \cdot 6H_2O$, KSCN, and KCl were prepared and placed in the wells of vacuum desiccators to create sealed systems with relative humidities respectively at 33, 47, and 86%. Before sealing these containers, several grids with epitaxially crystallized samples were placed face up (to expose the crystals to the ambient humidity) above the solution reservoirs and the samples were allowed to stay in this atmosphere at room temperature for 16 days before they were withdrawn for initial examination.

Electron diffraction

Selected area electron diffraction measurements were made at 100 kV with a JEOL JEM-100B electron microscope equipped with a side-entry goniometer stage. As usual [14], low beam dose conditions and a fast photographic emulsion (Kodak DEF-5) are used to minimize radiation damage to the specimen by the electron beam. Diffraction spacings in an electron diffraction pattern are calibrated against a gold Debye-Scherrer pattern photographed at identical magnetic lens settings used to examine the lipids. Electron diffraction intensities are obtained from scans of films made with a Joyce Loebl Mk III C flatbed microdensitometer.

Examination of anhydrous crystals in the electron microscope vacuum requires no special treatment. However, the diffraction of hydrated specimens was made possible by use of a Gatan 626 cooling stage for the electron microscope. As soon as the grid containing hydrated epitaxial crystals was removed from the humidity chamber, it was placed in the specimen capsule for the cooling stage and this assembly was plunged into liquid nitrogen in the well of the insulated chamber around the specimen holder for the cryostage. After mounting the capsule into the holder, a frost protection shield was slid over the specimen position on the rod and the precooled cryostage was then inserted into the electron microscope, after which the coolant in the stage Dewar was filled to the top. Although the specimen can be cooled to near −170 °C, the inefficiency of the anticontamination trap of the electron microscope does not permit visualization of the diffraction patterns without a contaminant ice diffraction pattern unless the specimen rod is heated above −91 °C. We used a tip temperature of −87 °C in these experiments which is stably maintained by the thermo-regulated power supply supplied with the specimen stage.

Low dose lattice images

Direct electron microscope images of the phospholipid lamellae were obtained from epitaxial crystals at low electron beam dose at an operational mag-

nification of 20,000× using the procedure of Fryer and Dorset [15]. This requires that the microscope is first corrected for astigmatism at much higher magnification (*e.g.* 100,000×) and pains are taken to reduce the exposure to the sample before photographing the crystal image. A highly underfocussed objective lens is used to emphasize phase contrast detail due to the low angle lamellar electron diffraction spots from these crystals.

The low dose images are then placed on an optical bench under laser illumination to determine the spatial resolution of the lamellar repeat structure which is directly visible on the film. After defining optimal image areas, these were scanned on an Optronics P1000 rotating drum densitometer at 25 μm raster to give a digitized pixel density representation of the image as a computer file. This can be manipulated by image processing software such as IMAGIC [16]. Phase values are found from the computed Fourier transform of the image at the center of the refined reciprocal lattice spots. The crystallographic phases can be easily retrieved after shifting the image to an allowed unit cell origin, since the bandpass of the phase contrast transfer function does not contribute appreciable phase errors in this region of reciprocal space.

Computations

For the analysis of the diffraction data presented below, a model for the 1,2-dimyristoyl-phosphatidylethanolamines is constructed based on the crystal structure of 1,2-dilauroyl-*rac*-glycerophosphoethanolamine-acetic acid [7] with appropriately lengthened acyl chains. The outermost acyl chain carbon is then placed at the unit cell fractional coordinate $z = 0.5$ and translational shifts Δz are made along the long axis for sequential calculation of kinematical structure factors according to the $P\bar{1}$ constraints to this reciprocal lattice row:

$$\left| F_{00\ell}^{\text{calc}} \right| = \sum_j f_j' \cos 2\pi(\ell z).$$

Here f_j' is the scattering factor (respectively X-ray or electron [17] depending on radiation source) corrected for thermal motion. Here we use the approximation of Hitchcock *et al.* [8] for the isotropic temperature factor

$$B = (4.0 + C + 108z^2)A^2$$

where z are the atomic fractional coordinates for the starting model. Comparative use is also made of the one-dimensional Patterson function defined

$$P(\text{w}) = \sum_j \left| F_{00\ell} \right|^2 \cos 2\pi(\ell z)$$

where the structure factor magnitude can either be an observed or calculated value. As is discussed extensively elsewhere [9], observed electron diffraction structure factor magnitudes are obtained from measured intensity data after a correction is made for crystal texture (lamellar curvature), hence:

$$\left| F_{00\ell}^{\text{obs}} \right| = \text{k}(\text{I}_{\text{obs}} \cdot \ell)^{1/2}. \quad (1)$$

Results

Reappraisal of X-ray diffraction studies

a. 1,2-Dimyristoyl-*rac*-glycerophosphoethanolamine (DL-DMPE)

Since the original structure analysis for the racemic dimyristoyl lipid based on lamellar X-ray data used a rather coarse translational shift increment [8], two nearby crystallographic residual minima were found only when a second analysis sampled the translational shifts at finer intervals [9]. Subsequent to this second analysis, it was found that the computer program used to calculate structure factors misapplied the isotropic thermal parameters. A new program, which has been checked for model structures by hand calculation, was used to re-evaluate these structure factors for DL-DMPE models at various translations past the unit cell origin. As shown in Fig. 1, the results of the analysis are essentially the same as before [9], probably because the low angle data are least sensitive to temperature factor attenuation of scattering factors. The only change is that the value for the deepest residual minimum is now $R = 0.12$, pointing to the correctness of this structural model. A comparison of Patterson functions for observed and calculated intensity data is shown in Fig. 2. If one assumes reasonably that a linear correlation must exist between these functions, then the computed correlation coefficient is $r = 1.00$. Calculated and observed structure factors are listed in Table I.

b. 1,2-dimyristoyl-*sn*-glycerophosphoethanolamine (L-DMPE)

In the paper by Suwalsky and Duk [10] observed diffraction intensities were corrected for a Lorentz

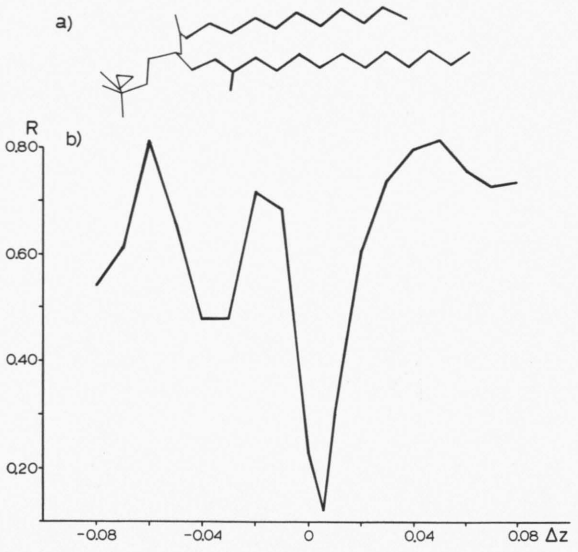

Fig. 1. (a) Molecular conformation of 1,2-dimyristoyl-glycerophosphoethanolamine used for translational structural searches with X-ray and electron lamellar diffraction intensities and based on the crystal structure of the racemic 1,2-dilauroyl homolog [7]. (b) Structural analysis of DL-DMPE using X-ray diffraction data in ref. [8]. Although not stated by the authors, it is clear, after inspection of the raw data in ref. [21], that a Lorentz correction of the type $|F_{00\ell}^{obs}| = (I_{00\ell}^{obs}\,\ell)^{1/2}$ was applied to the observed intensities. The lamellar repeat is d_{001} = 49.5 Å and the residual minimum in this analysis corresponds to one found previously [9].

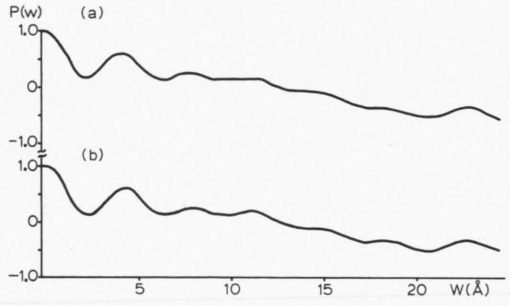

Fig. 2. Patterson functions for DL-DMPE calculated (a) from observed intensity data in ref. [8] and (b) from the calculated intensities for the model expressed by the residual minimum in Fig. 1b. The correlation coefficient for these two Patterson functions assuming a linear correlation is r = 1.00. Major intermolecular peaks are found at 4.0, 7.8 and 10.9 Å.

Table I. Calculated and observed structure factors for analyses of 1,2-dimyristoyl-phosphatidylethanolamine (relative values).

L-DMPE (e.d.)			L-DMPE (x.d.)			DL-DMPE (x.d.)		
ℓ	$\lvert F_o \rvert$	F_c	ℓ	$\lvert F_o \rvert$	F_c	ℓ	$\lvert F_o \rvert$	F_c
1	1.38	1.92	1	4.84	9.17	1	13.49	13.15
2	1.59	−0.24	2	1.70	1.75	2	2.04	2.36
3	0.87	−0.40	3	2.99	0.24	3	2.50	−0.10
4	1.36	−1.44	4	3.48	−3.24	4	5.26	−4.82
5	0.89	−0.79	5	1.95	−1.18	5	1.05	−1.93
6	0.78	−0.88	6	0.73	−1.16	6	1.95	−1.81
7	0.82	−0.83	7	3.00	−1.08	7	1.70	−1.74
8	0.44	−1.03	8	1.62	−2.04	8	1.75	−2.96
9	0.90	−1.51	9	1.64	−3.75	9	4.29	−4.78
10	1.34	−1.42	10	5.15	−3.44	10	3.76	−4.26
11	2.04	−2.05	11	4.92	−5.07	11	5.53	−5.62
12	1.47	−1.55	12	5.17	−4.21	12	4.43	−4.43
13	1.44	−1.96	13	4.94	−6.28	13	6.00	−5.87
14	1.40	−0.68	14	4.96	−4.74	14	3.73	−3.89
			15	3.57	−3.31	15	2.46	−2.21
R = 0.31			R = 0.35			R = 0.12		

and polarization factor consistent with standard procedure for powder X-ray diagrams [18] *i.e.*

$$|F_o| = (I_o/L_p)^{1/2}$$

where $L_p = \dfrac{1 + \cos^2(2\theta)}{\sin 2\theta}$.

For reasons not mentioned by these authors, the product of a thermal parameter $T = \exp(-B\sin^2\theta/\lambda^2)$ was then made with this correction, where B = 3.0 Å^2. Since this is not a usual procedure in X-ray crystallography, we have regenerated the raw observed intensity magnitudes from the structure factor values listed in their Fig. 2 [10] and have recorrected the intensities for crystal texture according to Eqn. (1) above, which is often used for the X-ray crystallography of oriented lipid lamellae [19].

The conformational model used for the structure analysis of DL-DMPE was again used in a translational structure search for which the residual minima between computed structure factors and corrected observed data were determined. As shown in Fig. 3a, the position of these minima are at nearly the same places as in the previous analysis, although the value R = 0.36 is rather high. A comparison of Patterson functions computed from observed corrected intensities and the calculated intensities for the best residual minimum is given in Fig. 4. The correlation coefficient computed from the linear comparison of these maps is r = 0.77. Calculated and observed structure

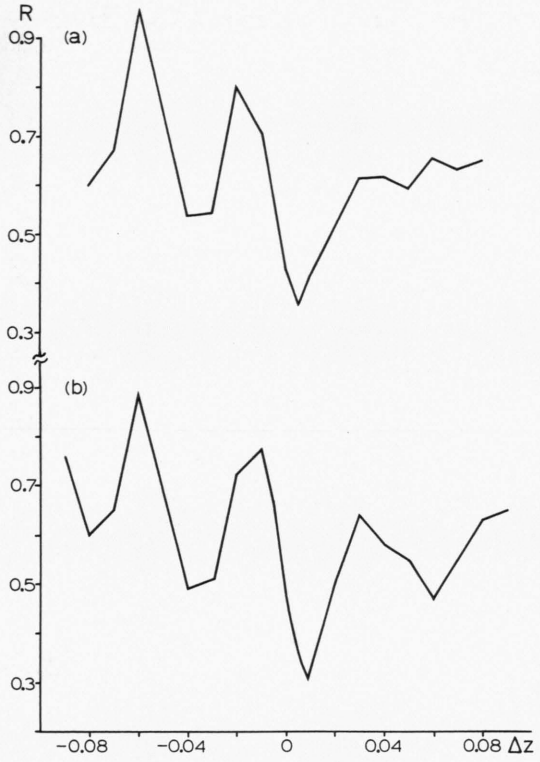

Fig. 3. Translational structure searches for L-DMPE based: (a) on X-ray diffraction data in ref. [10]. The lamellar spacing is d_{001} = 50.25 Å; (b) on electron diffraction data obtained from epitaxially crystallized microcrystals. The lamellar spacing is d_{001} = 51.00 ± 0.56 Å. In either case the residual minimum nearly corresponds to the same structure solution found for the racemic material (Fig. 1b).

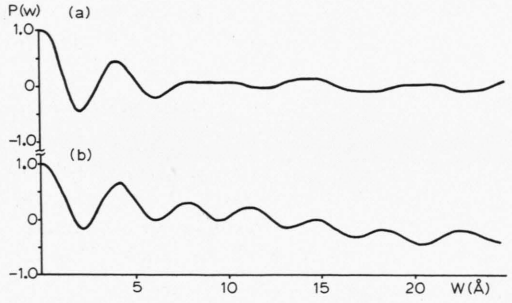

Fig. 4. Patterson functions for L-DMPE based on X-ray intensity data. (a) Observed data from ref. [10]. Major peak centers are located at 4.0, 7.9 and 10.0 Å (the latter being a shoulder of a rather broad peak). (b) Calculated data for model at the residual minimum indicated in Fig. 3a. As shown by the poor correlation coefficient for the regression line relating the Patterson functions (r = 0.77), the agreement between the model structure and the observed diffraction data is worse than for the racemic compound (Fig. 1, 2).

factors are listed in Table I. Note that the phase values are not in accord with the earlier analysis [10].

Electron diffraction structure analysis

Because the agreement between calculated and observed electron diffraction structure factor magnitudes for L-DMPE was rather poor in a previous analysis [9], new lamellar intensity data (Fig. 5a) from the chiral lipid was obtained from thinner epitaxially oriented crystals. After appropriate correc-

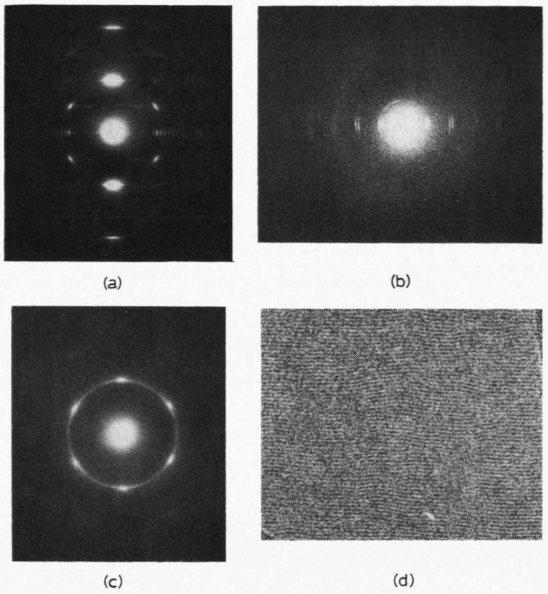

Fig. 5. Electron diffraction data from L-DMPE: (a) Anhydrous crystals epitaxially crystallized on naphthalene. Although at first glance this resembles a two-dimensional reciprocal net, the pattern is actually a superposition of the lamellar 00ℓ pattern produced by epitaxy (d_{001} = 51.00 ± 0.56 Å) and a subcell pattern in a view down the acyl chains corresponding to axial dimensions d_{100} = 7.60 ± 0.12 Å and d_{010} = 9.46 ± 0.10 Å. Although the intensities have not been used to quantitatively verify the subcell packing, the most intense hk0 reflections in the pattern strongly resemble those from solution grown DL-DPPE [11] and are undoubtedly due to the hybrid orthorhombic subcell HS1 [29]. (b) Water-swollen epitaxial crystals. The lamellar 00ℓ row is doubled, thus revealing the coexistence of the anhydrous and hydrated form. The ratio of lamellar spacings ($d_{\text{hydrated}}/d_{\text{anhydrous}}$ = 1.03) is very similar to the value found by Suwalsky and Duk [10] (1.02). (c) Solution crystallized crystals showing the existence of an alternate chain packing (hexagonal subcell d_{100} = 4.18 ± 0.02 Å) found also for the racemic form [11]. (d) Low-dose phase contrast electron microscope lattice image of L-DMPE used for determination of low angle crystallographic phases *via* image processing.

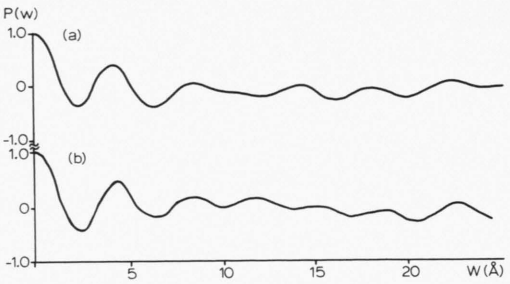

Fig. 6. Comparison of Patterson functions computed with lamellar electron diffraction data from epitaxially crystallized L-DMPE: (a) observed data, major peak positions at 4.0, 8.4 and 10.0 Å (the latter peak is a shoulder), (b) calculated data from the best model in the analysis of Fig. 3b. The correlation coefficient for the two Patterson functions assuming linear correlation is $r = 0.87$.

tions (see above) these data were used in the same translational structure analysis as carried out above (with appropriately changed scattering factors). The results of this analysis (Fig. 3b) shows that the lowest residual minimum ($R_{min} = 0.31$) lies at the same position as found in the previous X-ray analyses. A comparison of Patterson functions is depicted in Fig. 6. The correlation coefficient for the regression line relating the Patterson functions computed from observed and model data is $r = 0.87$. A listing of calculated and observed structure factor values for the structural analyses is given in Table I. The phase assignments for the first two reflections agree with the values determined from the analysis of direct low dose e.m. lattice images (Fig. 5d).

An electron diffraction pattern from water-swollen lamellar crystals is shown in Fig. 5b. As found in the earlier X-ray analysis [10] there appears to be a limiting value for water uptake by the phosphatidylethanolamine and the increase in lamellar spacing also agrees with the previously measured value [10]. A plot of relative structure factor magnitudes from two swelling experiments indicates that not much of the continuous transform of the unit cell is sampled in this swelling experiment (Fig. 7c).

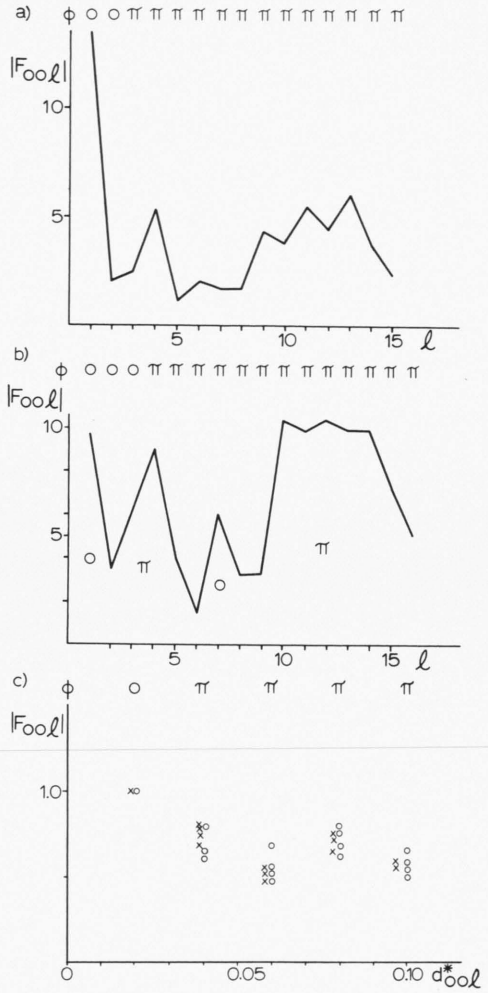

Fig. 7. Structure factor magnitudes for DMPE: (a) X-ray data for the racemic compound [8] with phase assignments found in our structure analysis (Table I), (b) X-ray data for the chiral compound [10] with phase assignments suggested by our structure analysis compared to values assigned in a previous analysis [10]. (c) Swelling data from our electron diffraction study (peak heights) with phase values found in our structure analysis. Note that the magnitude $|F_{001}| > |F_{002}|$ in this plot disagrees with $|F_{001}| < |F_{002}|$ listed in Table I. Although the former relationship is most commonly found, correction of the values in Table I for presumed multiple scattering [14] does not affect the value of the R-factor minimum significantly.

Discussion

For the comparison of optically active and racemic phosphatidylethanolamines, it is first important to establish that nearly the same crystal packing made up of untilted molecules is represented in either compound, since polymorphism involving chain tilt has been observed in this lipid class [20]. The near congruency of lamellar spacings is the major evidence for this assumption, as shown by several laboratories [9, 21]. The unit cell lengths normal to this lamellar direction, on the other hand, are slightly

different for the two compounds. An electron diffraction determination [11] of the hybrid orthorhombic subcell axes for DL-DPPE (a_s = 7.76, b_s = 10.03 Å) is very close to the respective unit cell axes found for DL-DLPE [7] but represents a 3 to 4% expansion of the distances found for the optically active form [10] (a_s = 7.45, b_s = 9.70 Å). Our measurements of electron diffraction HS1 subcell spacings for appropriately oriented crystals coexisting with epitaxially crystallized L-DMPE (Fig. 5a), *i.e.*, d_{200} = 3.80 ± 0.06 Å, d_{020} = 4.73 ± 0.05 Å, also support the conclusion that the lateral spacings are shorter for the chiral material. From a comparison of Patterson functions computed from observed X-ray intensities (see Fig. 2, 4), both optically active and racemic materials have major intermolecular vectors near 4.0, 8.0 and 10–11 Å, indicating similar headgroup conformations, following the analytical procedure of Khare and Worthington [22]. On the other hand, the correlation coefficient for the regression line relating the two respective Patterson functions computed from observed data is only r = 0.63. The fit of observed X-ray lamellar structure factors is likewise poor (R = 0.42). (Before this comparison was made, it was ascertained that sets of X-ray intensity data from L-DMPE and DL-DMPE were corrected for sample texture in the same way. A suspicion that the I_{001} for L-DMPE might be underestimated only gave a modestly improved fit of the two data sets (R = 0.36), after this reflection was discarded from the comparison.)

Although some structural similarities may be deduced from the X-ray analyses for the two compounds, there are also reasons to believe that differences in crystal packing are present. Where exactly this structural difference would be found is presently difficult to determine. The electron diffraction structure analysis described above again supports the basic conformational similarity for the optically active and racemic forms. A neutron diffraction analysis on the chiral dipalmitoyl homolog [23] also points to the similarity of the polar group conformations for these compounds [24]. Since the lamellar spacings are also nearly identical, the major difference must be mainly due to the slight expansion in the in-plane packing distance of the racemic crystal. Ordinarily, a decrease in packing density (here about 6%) also indicates an *increase* in potential energy for the crystal [25] and thus one would expect the racemic compound to melt lower than the chiral form. The opposite melting behavior possibly points to the well-known stability of a hydrogen bond network in the racemic molecular packing [26] (thus accounting for the slight lateral expansion in headgroup packing) which is not found in the chiral material. The importance of this energetic contribution to the internal energy could be similar to the case of the alkyl amides which causes them to deviate from the melting point convergence behavior expected for alkane chain derivatives [27]. Just what slight conformational changes are needed to account for the slightly different headgroup packing of the chiral material in the direction of the lamellar repeat must be reserved for another study – *e.g.* an electron diffraction of L-DPPE and DL-DPPE, both of which are still commercially available. An initial attempt to answer this question with models based on the two headgroup conformations of DMPC [28], did not arrive at an improved headgroup packing model for L-DMPE, either with X-ray or with electron diffraction data.

The above analysis unfortunately shows that the use of lamellar X-ray data from unswollen or minimally hydrated phospholipid monolayers for phase determination [10] in the same way as data from continuously hydrated multilayers, *e.g.* of lecithins [7], are used, may not be a very accurate method. For example, the corrected X-ray structure factors magnitudes for L-DMPE are plotted in Fig. 7b with the phase assignments made on the basis of presumed "node" positions in the continuous unit cell transform [26]. By comparison to a well determined structure (Fig. 7a) the X-ray structure factor magnitudes for DL-DMPE are shown to have node positions which could correspond approximately to those for the chiral compound. Yet, only the first node represents a real change in phase sign, as seen from the successful translational structure search with a molecular model. The effect of phasing procedure on the appearance of the electron density map is depicted in Fig. 8.

The results of our swelling series for L-DMPE studied in the electron microscope are plotted in Fig. 7c. It would be difficult to know where to locate a change in phase value in such a plot because the relative structure factor magnitudes from hydrated structures are not much different from the unhydrated form.

On the other hand, it is significant to note in the electron diffraction study that the epitaxial orientation of phospholipid molecules can be preserved

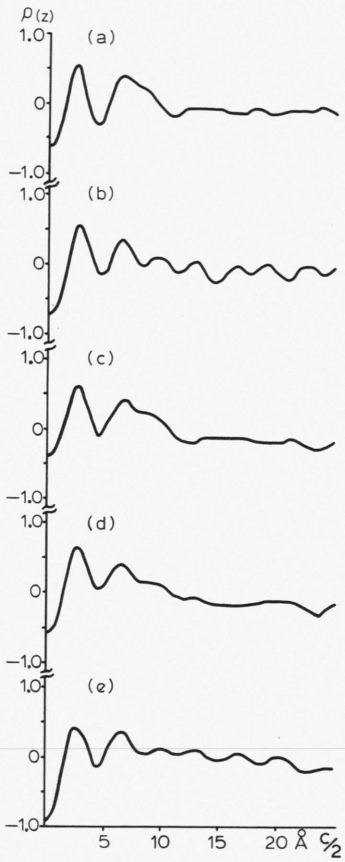

during such a dynamic swelling experiment similar to the allowable translational shifts demonstrated already for thermotropic transitions to the smectic phase [6]. Thus, electron diffraction structure analysis should be a valuable technique for future hydration studies of more hygroscopic materials such as the phosphatidylcholines.

Acknowledgements

The author is grateful to the Manufacturers and Traders Trust Company for a grant to support this research.

Fig. 8. One-dimensional electron density maps for 1,2-dimyristoyl-phosphatidylethanolamine: (a) L-DMPE phase set of Suwalsky and Duk [10], (b) L-DMPE phase set in Table I, (c) DL-DMPE phase set with criteria similar to (a), (d) DL-DMPE, phase set in Table I. One-dimensional electrostatic potential map (e) L-DMPE, phase set in Table I. For all maps above, the density values are on a relative scale.

[1] A. I. Kitaigorodskii, Mixed Crystals, pp. 39–40, 248ff., Springer Verlag, Berlin 1984.
[2] M. Iwahashi, K. Ashizawa, M. Ashizawa, Y. Kaneko, and M. Muramatsu, Bull. Chem. Soc. Japan **57,** 956 (1984).
[3] A. I. Boyanov, R. D. Koynova, and B. G. Tenchov, Chem. Phys. Lipids **39,** 155–163 (1986).
[4] I. Sakurai, S. Sakurai, T. Sakurai, T. Seto, A. Ikegami, and S. Iwayanagi, Chem. Phys. Lipids **26,** 41 (1980).
[5] I. Sakurai, T. Sakurai, T. Seto, and S. Iwayanagi, Chem. Phys. Lipids **32,** 1 (1983).
[6] D. L. Dorset and A. K. Massalski, Biochim. Biophys. Acta **903,** 319 (1987).
[7] M. Elder, P. Hitchcock, R. Mason, and G. G. Shipley, Proc. Roy. Soc. (London) **A 354,** 157 (1977).
[8] P. B. Hitchcock, R. Mason, and G. G. Shipley, J. Mol. Biol. **94,** 297 (1975).
[9] D. L. Dorset, A. K. Massalski, and J. R. Fryer, Z. Naturforsch. **42a,** 381 (1987).
[10] M. Suwalsky and L. Duk, Makromol. Chem. **188,** 599 (1987).
[11] D. L. Dorset, Biochim. Biophys. Acta **424,** 396 (1976).
[12] J. C. Wittmann and R. St. John Manley, J. Polym. Sci., Polym. Phys. Ed. **16,** 1891 (1978).
[13] D. L. Dorset, W. A. Pangborn, and A. J. Hancock, J. Biochem. Biophys. Methods **8,** 29 (1983).
[14] D. L. Dorset, J. Electron Microsc. Techn. **2,** 89 (1985).
[15] J. R. Fryer and D. L. Dorset, J. Microsc. (Oxford) **145,** 61 (1987).
[16] M. v. Heel and W. Keegstra, Ultramicroscopy **7,** 113 (1981).
[17] P. A. Doyle and P. S. Turner, Acta Cryst. **A 24,** 390 (1968).
[18] L. E. Alexander, X-Ray Diffraction Methods in Polymer Science, p. 41, Krieger, Mulabar, Florida 1985.
[19] N. P. Franks, J. Mol. Biol. **100,** 345 (1976).
[20] M. Suwalsky and E. Knight, Z. Naturforsch. **37c,** 1157 (1982).
[21] J. P. Green, M. C. Phillips, and G. G. Shipley, Biochim. Biophys. Acta **330,** 243 (1973).
[22] R. S. Khare and C. R. Worthington, Biochim. Biophys. Acta **514,** 239 (1978).
[23] G. Büldt and J. Seelig, Biochemistry **19,** 6170 (1980).
[24] G. Büldt and R. Wohlgemuth, J. Membrane Biol. **58,** 81 (1981).

[25] A. I. Kitaigorodskii, Organic Chemical Crystallography, p. 109ff., p. 179, Consultant's Bureau, New York 1961.
[26] I. Pascher, S. Sundell, and H. Hauser, J. Mol. Biol. **153,** 807 (1981).
[27] J. Torbet and M. H. F. Wilkins, J. Theor. Biol. **62,** 447 (1976).
[28] R. H. Pearson and I. Pascher, Nature **281,** 499 (1979).
[29] S. Abrahamsson, B. Dahlén, H. Löfgren, and I. Pascher, Progr. Chem. Fats Other Lipids **16,** 125 (1978).